Published in final edited form as:
Science. 2012 June 8; 336(6086): 1317–1321. doi:10.1126/science.1220030.

Chemokine gene silencing in decidual stromal cells limits T cell access to the maternal-fetal interface

Patrice Nancy[1], **Elisa Tagliani**[1], **Chin-Siean Tay**[1], **Patrik Asp**[2,3], **David E. Levy**[1,2], and **Adrian Erlebacher**[1,2]

[1]Department of Pathology, New York University School of Medicine, New York, NY, 10016, USA

[2]NYU Cancer Institute, New York University School of Medicine, New York, NY, 10016, USA

Abstract

The chemokine-mediated recruitment of effector T cells to sites of inflammation is a central feature of the immune response. The extent to which chemokine expression levels are limited by the intrinsic developmental characteristics of a tissue has remained unexplored. We show in mice that effector T cells cannot accumulate within the decidua, the specialized stromal tissue encapsulating the fetus and placenta. Impaired accumulation was in part attributable to the epigenetic silencing of key T cell-attracting inflammatory chemokine genes in decidual stromal cells, as evidenced by promoter accrual of repressive histone marks. These findings give insight into mechanisms of fetomaternal immune tolerance as well as reveal the epigenetic modification of tissue stromal cells as a modality for limiting effector T cell trafficking.

Besides being essential for reproductive success, the ability of the allogeneic fetus and placenta to avoid rejection by the maternal immune system during pregnancy (i.e. fetomaternal tolerance) has served as a paradigm for the study of organ-specific immune tolerance (1). Recent work on this problem has made use of the Act-mOVA mating system, in which wild-type female mice crossed with males hemizygous for the Act-mOVA transgene (2) generate concepti expressing a transmembrane form of the model antigen chicken egg ovalbumin (OVA) from the ubiquitously active β-*actin* promoter (3, 4). As early as embryonic day (E) 7.5, OVA is expressed at high levels by trophoblasts directly contacting the uterus (i.e. at the maternal/fetal interface) (3), thus exposing maternal tissue to a surrogate fetal/placental antigen that should in principle allow for T cell priming and render the conceptus susceptible to attack by antigen-specific cytotoxic T lymphocytes (CTLs).

This mating system has been used to show that fetal rejection is in part prevented by mechanisms that minimize the activation of naïve T cells with fetal/placental specificity (3, 5). However, antigen-specific fetal loss still does not occur when systemic anti-fetal/placental CTL activity is experimentally induced in late gestation (3). Thus, a fail-safe mechanism also exists to protect the conceptus from activated CTLs. To visualize this

Address for correspondence: Adrian Erlebacher, Department of Pathology, New York University School of Medicine, Langone Medical Center, Smilow Research Building, Room 311, 550 First Avenue New York, NY 10016, (212) 263-8926 tel, (212) 263-8211 fax, adrian.erlebacher@nyumc.org.
[3]Current address: Liver Transplant Program, Montefiore Medical Center, Albert Einstein College of Medicine, Bronx, NY, 10467, USA

Supporting Online Material
Materials and Methods
Figs. S1 to S7
References (*20–29*)

phenomenon more directly, we asked whether pregnant mice, immunized with soluble OVA prior to mating, would show Act-mOVA-specific fetal loss on E10.5 after being rechallenged with OVA plus adjuvant (agonistic CD40 antibodies plus poly(I:C)) on E5.5 (6). We studied this period of early gestation because the behavior of OVA-specific T cells would not be influenced by the systemic release of fetal/placental OVA, which starts on ~E10.5 (3). Strikingly, pregnant mice bore the expected Mendelian proportion of Act-mOVA$^+$ concepti (17 of 26 total embryos from n=3 pregnant mice), even though 14–20% of splenic CD8 T cells were OVA-specific at the time of sacrifice (fig. S1). Thus, fetal rejection does not occur even when memory T cells with known fetal/placental specificity are reactivated in early pregnancy.

To find possible explanations for this observation, we evaluated the distribution of reactivated memory T cells in the uteri of C57BL/6-mated mice. Consistent with the ability of effector T cells to infiltrate peripheral tissues even in the absence of a localized antigen source (7, 8), E8.5 mice re-challenged with OVA plus adjuvant on E5.5 showed large numbers of CD3$^+$ T cells distributed throughout the segments of myometrium (and associated submyometrial stroma) overlying each implantation site (Fig. 1, A and B), as well as throughout the myometrium and endometrium of the undecidualized uterine segments between implantation sites (i.e. inter-implantation sites; Fig. 1, C and D). In contrast, CD3$^+$ cells in the decidua appeared sparse (Fig. 1B), with tissue densities remaining at levels similar to those seen throughout the uteri of mice that were not OVA-rechallenged. CD3$^+$ cells in the decidua were most prominent within blood vessels; however, most were extravascular in the implantation site-associated myometrium and inter-implantation sites (Fig. 1E, F). Together, these results suggested that the decidua had a reduced capacity for T cell accumulation, possibly due an intrinsic inability to recruit T cells from the blood. Accordingly, reactivated memory T cells were also unable to infiltrate decidual tissue encapsulating OVA-expressing concepti (fig. S2), or in hormonally pseudopregnant females with oil-induced artificial deciduomas (see Fig. 4).

Because anti-CD40 antibodies plus poly(I:C) induce a type 1-polarized T cell response (9), we tested whether impaired decidual T cell infiltration was due to low expression of T helper 1(Th1)/T cytotoxic 1 (Tc1) chemoattractants. Strikingly, 6 h after the intravenous injection of anti-CD40 antibodies, poly(I:C), and endotoxin-contaminated OVA, a regimen expected to increase blood levels of the pro-inflammatory cytokines tumor necrosis factor-α (TNFα) and interferon-γ (IFNγ) (10, 11), high levels of the key Th1/Tc1-attracting chemokine CXCL9 (a CXCR3 ligand) (12) were apparent in the segments of myometrium overlying each E8.5 implantation site (Fig. 2, A and B). In contrast, much lower CXCL9 expression was apparent in the decidua. High CXCL9 expression was also induced in both the endometrium and myometrium of the undecidualized uteri of pseudopregnant females (fig. S3), with the vast majority of the expressing cells being CD45$^-$ stromal cells (Fig. 2C). Because endometrial stromal cells (ESCs) are the precursors of decidual stromal cells (DSCs), the major cell type of the decidua, these results suggested that the developmental process of decidualization reduced the cells' capacity to produce T cell chemoattractants under inflammatory conditions.

We next independently prepared highly enriched stromal cells from E7.5 artificial deciduomas and overlying myometrium (fig. S4) and evaluated their inflammatory response *in vitro* (Fig. 2D). As with other cell types (13, 14), myometrial stromal cells (MSCs) treated with a combination of TNFα and IFNγ showed synergistic mRNA induction of both *Cxcl9* and *Cxcl10*, which encodes a second CXCR3 ligand. Furthermore, *Ccl5*, whose product CCL5 (RANTES) has also been implicated in Th1/Tc1 recruitment to inflamed tissues (12), was upregulated ~15-fold in TNFα-treated MSCs, with expression further augmented by IFNγ. In contrast, *Ccl5* and *Cxcl9* transcript levels in DSCs remained unchanged after

cytokine treatment, whereas TNFα+IFNγ mildly induced *Cxcl10* expression to levels that barely exceeded those of MSCs at baseline. The expression pattern of *Cxcl11*, which encodes the third known CXCR3 ligand, was similar to that of *Cxcl9* and *Cxcl10* (fig. S5). The inability of DSCs to produce Th1 chemoattractants was functionally confirmed using transwell migration assays, which furthermore showed that MSCs attract Th1 cells through the induction of CXCR3 ligands and CCL5 (Fig. 2E, F). Together, these results suggested that the inability of DSCs to produce T cell-attracting chemokines under inflammatory conditions *in vivo* was due to a cell-intrinsic defect in their inflammatory cytokine response.

The inability of DSCs to produce CXCR3 ligands and CCL5 was not explained by decreased activation of NF-κB or STAT1, the major transcription factors mediating TNFα and IFNγ signaling (fig. S6A, B). Moreover, we could find examples of NF-κB and STAT1 target genes that were induced in DSCs in a relatively robust fashion (fig. S6C). These results suggested that the DSC chemokine expression defects were gene-specific and independent of inflammatory signaling *per se*. We therefore evaluated gene-specific chromatin configurations using chromatin immunoprecipitation (ChIP) assays. Elevated basal levels of the repressive histone H3 trimethyl lysine 27 (H3K27me3) mark (15) were present on the *Cxcl9* and *Cxcl10* promoters in DSCs as compared to MSCs (Fig. 3A, top row). Conversely, TNFα+IFNγ treatment increased *Cxcl9/10* promoter levels of acetylated histone H4 (H4Ac), a mark of active gene transcription, in MSCs but not DSCs (Fig. 3A, bottom row). Both cell populations showed the inverse patterns of H3K27me3 and H4Ac occupancies on the *Gapdh* and *Cd8a* promoters expected from these genes' respectively high and low constitutive expression levels. Thus, low cytokine inducibility of *Cxcl9/10* in DSCs was associated with the gene-specific presence of the repressive H3K27me3 histone mark.

In vivo ChIP assays performed directly on dissected E7.5 uterine tissue layers also revealed high levels of the H3K27me3 mark on the *Cxcl9/10* promoters in whole decidua as compared to overlying myometrium, thus demonstrating that *Cxcl9/10* silencing was also a feature of true, pregnancy-associated decidua *in vivo* (Fig. 3B). Recognizing that undecidualized uteri are comprised equally in volume by endometrium and myometrium (5), this result also meant that *in vivo* ChIP assays could be used to infer chromatin configurations in undecidualized ESCs, as these cells could not be sufficiently purified for *ex vivo* assays. Accordingly, *Cxcl9/10* H3K27me3 promoter occupancies in whole non-pregnant uteri and E7.5 inter-implantation sites were similar to those in segments of implantation site-associated myometrium, and clearly not intermediate between the myometrium and decidua (Fig. 3B). This result strongly suggested that the H3K27me3 modification of the *Cxcl9/10* promoters appears upon transformation of ESCs into DSCs.

The *Ccl5* promoter also showed increased H3K27me3 occupancy in whole decidua as compared to myometrium and undecidualized uterus (Fig. 3B), suggesting a shared pathway for minimizing decidual chemokine expression. Interestingly, this increase was not readily apparent *ex vivo*, while H3K27me3 levels on the *Cxcl9/10* promoters appeared somewhat reduced upon TNFα+IFNγ treatment (Fig. 3A). These results suggest some level of reversibility of the H3K27me3 mark at the locations we assessed by ChIP, possibly as a result of just isolating and culturing the cells. Since H4Ac levels on the *Cxcl9/10* and *Ccl5* promoters were nonetheless unchanged in TNFα+IFNγ-treated DSCs (Fig. 3A), it is likely that the continued repressed status of these genes after 24 h culture also involves either the presence of the H3K27me3 mark in other regions of their respective loci, or the presence of other repressive modifications.

We next determined the effect of ectopic chemokine expression within the decidua by injecting artificial deciduomas in OVA-rechallenged mice with control, *Cxcl9*, or *Ccl5*-expressing lentiviruses mixed with EGFP reporter lentiviruses. For each mouse, decidual

$CD3^+$ T cell densities were normalized to myometrial $CD3^+$ cell densities in order to account for systemic differences in the magnitude of the anti-OVA T cell response. $CD3^+$ cell densities in the GFP^+ decidual areas of control virus-injected mice were elevated as compared to uninfected, GFP^- decidual areas, thus revealing a non-specific effect of viral infection *per se*. However, these densities were not further altered in mice injected with *Cxcl9*- or *Ccl5*-expressing viruses. In contrast, $CD3^+$ cell densities in decidual areas infected with mixtures of *Cxcl9*- and *Ccl5*-expressing viruses were significantly elevated compared to control virus-infected areas (Fig. 4). The synergistic effect of dual CXCL9/CCL5 expression thus apparent is consistent with recent observations in a malignant melanoma model (16). Furthermore, since CXCL9 expression in *Cxcl9*+*Ccl5*-infected decidual areas was undetectable by tissue immunostaining (fig. S7), it was unlikely that T cell infiltration into these areas was due to supra-physiologic chemokine expression. Together, these results suggested that inadequate endogenous expression of CXCR3 ligands and CCL5 was limiting for decidual T cell accumulation.

Provocatively, T cells have been reported to be relatively scarce in the human decidua (17, 18), implicating the developmental program of decidual chemokine silencing described here as a potentially conserved mechanism of fetomaternal tolerance. Consistent with this possibility, *Cxcl10* is expressed only focally in the human decidua, in association with peri-glandular leukocyte aggregates (19). As the presence of even low numbers of activated T cells at the maternal/fetal interface might disturb placental development or function, dysregulation of this pathway might also contribute to a variety of pregnancy complications. Conversely, altered chemokine silencing may influence the susceptibility of the decidua to infection. More generally, however, our results demonstrate that genes encoding Th1/Tc1 attracting chemokines are subject to epigenetic regulation in tissue stromal cells, and that such regulation can significantly influence a tissue's capacity for T cell accumulation. This demonstration raises questions regarding how the repressive H3K27me3 histone mark is targeted to select chemokine genes, and whether related pathways control T cell access to the stroma of infected, autoimmunity-afflicted, or cancer-bearing tissues.

Supplementary Material

Refer to Web version on PubMed Central for supplementary material.

Acknowledgments

We thank S. K. Dey and K. Johnson for advice, and A. Frey and J. Ernst for comments on the manuscript. The Histopathology and Vaccine & Cell Therapy core facilities of the NYU Cancer Institute provided histology services and tetramer reagents, and were supported by NIH–NCI (P30CA016087). P.N., E.T. and C.-S. T. performed experiments, P.A. and D.E.L. provided critical expertise and reagents, P.N. and A.E. analyzed data, P.N. and A.E. designed experiments and wrote the manuscript. The data reported in the manuscript are tabulated in the main paper and in the supplementary materials. Supported by grants from the NIH (RO1AI062980) and the American Cancer Society to A.E. (RSG-10-158-01-LIB).

Abbreviations

H3K27me3	histone H3 trimethyl lysine 27
H4Ac	acetylated histone H4
CTL	cytotoxic T lymphocyte
OVA	ovalbumin
myo	myometrium

dec	decidua
ESC	endometrial stromal cell
DSC	decidual stromal cell
MSC	myometrial stromal cell

References and notes

1. Trowsdale J, Betz AG. Mother's little helpers: mechanisms of maternal-fetal tolerance. Nat Immunol. 2006 Mar.7:241. [PubMed: 16482172]
2. Ehst BD, Ingulli E, Jenkins MK. Development of a novel transgenic mouse for the study of interactions between CD4 and CD8 T cells during graft rejection. Am J Transplant. 2003 Nov. 3:1355. [PubMed: 14525595]
3. Erlebacher A, Vencato D, Price KA, Zhang D, Glimcher LH. Constraints in antigen presentation severely restrict T cell recognition of the allogeneic fetus. J Clin Invest. 2007 May.117:1399. [PubMed: 17446933]
4. Moldenhauer LM, et al. Cross-presentation of male seminal fluid antigens elicits T cell activation to initiate the female immune response to pregnancy. J Immunol. 2009 Jun 15.182:8080. [PubMed: 19494334]
5. Collins MK, Tay CS, Erlebacher A. Dendritic cell entrapment within the pregnant uterus inhibits immune surveillance of the maternal/fetal interface in mice. J Clin Invest. 2009 Jun 22.119:2062. [PubMed: 19546507]
6. Materials and methods are available as supporting material on *Science* Online.
7. Reinhardt RL, Bullard DC, Weaver CT, Jenkins MK. Preferential accumulation of antigen-specific effector CD4 T cells at an antigen injection site involves CD62E-dependent migration but not local proliferation. J Exp Med. 2003 Mar 17.197:751. [PubMed: 12629067]
8. Masopust D, et al. Activated primary and memory CD8 T cells migrate to nonlymphoid tissues regardless of site of activation or tissue of origin. J Immunol. 2004 Apr 15.172:4875. [PubMed: 15067066]
9. Ahonen CL, et al. Combined TLR and CD40 triggering induces potent CD8+ T cell expansion with variable dependence on type I IFN. J Exp Med. 2004 Mar 15.199:775. [PubMed: 15007094]
10. Erlebacher A, Zhang D, Parlow AF, Glimcher LH. Ovarian insufficiency and early pregnancy loss induced by activation of the innate immune system. J Clin Invest. 2004 Jul.114:39. [PubMed: 15232610]
11. Longhi MP, et al. Dendritic cells require a systemic type I interferon response to mature and induce CD4+ Th1 immunity with poly IC as adjuvant. J Exp Med. 2009 Jul 6.206:1589. [PubMed: 19564349]
12. Bromley SK, Mempel TR, Luster AD. Orchestrating the orchestrators: chemokines in control of T cell traffic. Nat Immunol. 2008 Sep.9:970. [PubMed: 18711434]
13. Ohmori Y, Hamilton TA. The interferon-stimulated response element and a kappa B site mediate synergistic induction of murine IP-10 gene transcription by IFN-gamma and TNF-alpha. J Immunol. 1995 May 15.154:5235. [PubMed: 7730628]
14. Hiroi M, Ohmori Y. The transcriptional coactivator CREB-binding protein cooperates with STAT1 and NF-kappa B for synergistic transcriptional activation of the CXC ligand 9/monokine induced by interferon-gamma gene. J Biol Chem. 2003 Jan 3.278:651. [PubMed: 12403783]
15. Margueron R, Reinberg D. The Polycomb complex PRC2 and its mark in life. Nature. 2011 Jan 20.469:343. [PubMed: 21248841]
16. Hong M, et al. Chemotherapy induces intratumoral expression of chemokines in cutaneous melanoma, favoring T-cell infiltration and tumor control. Cancer Res. 2011 Nov 15.71:6997. [PubMed: 21948969]
17. Marlin R, et al. Decidual soluble factors participate in the control of HIV-1 infection at the maternofetal interface. Retrovirology. 2011; 8:58. [PubMed: 21767373]

18. Bulmer JN, Williams PJ, Lash GE. Immune cells in the placental bed. Int J Dev Biol. 2010; 54:281. [PubMed: 19876837]

19. Red-Horse K, Drake PM, Gunn MD, Fisher SJ. Chemokine ligand and receptor expression in the pregnant uterus: reciprocal patterns in complementary cell subsets suggest functional roles. Am J Pathol. 2001 Dec.159:2199. [PubMed: 11733370]

20. Abramoff MD, Magelhaes PJ, Ram SJ. Image processing with Image J. Biophotonics International. 2004; 11:36.

21. Weinmann AS, Bartley SM, Zhang T, Zhang MQ, Farnham PJ. Use of chromatin immunoprecipitation to clone novel E2F target promoters. Mol Cell Biol. 2001 Oct.21:6820. [PubMed: 11564866]

22. Frank SR, Schroeder M, Fernandez P, Taubert S, Amati B. Binding of c-Myc to chromatin mediates mitogen-induced acetylation of histone H4 and gene activation. Genes Dev. 2001 Aug 15.15:2069. [PubMed: 11511539]

23. Ghisletti S, et al. Cooperative NCoR/SMRT interactions establish a corepressor-based strategy for integration of inflammatory and anti-inflammatory signaling pathways. Genes Dev. 2009 Mar 15.23:681. [PubMed: 19299558]

24. Adelman K, et al. Immediate mediators of the inflammatory response are poised for gene activation through RNA polymerase II stalling. Proc Natl Acad Sci U S A. 2009 Oct 27.106:18207. [PubMed: 19820169]

25. Naldini L, Blomer U, Gage FH, Trono D, Verma IM. Efficient transfer, integration, and sustained long-term expression of the transgene in adult rat brains injected with a lentiviral vector. Proc Natl Acad Sci U S A. 1996 Oct 15.93:11382. [PubMed: 8876144]

26. Qin XF, An DS, Chen IS, Baltimore D. Inhibiting HIV-1 infection in human T cells by lentiviral-mediated delivery of small interfering RNA against CCR5. Proc Natl Acad Sci U S A. 2003 Jan 7.100:183. [PubMed: 12518064]

27. Sierro F, et al. Disrupted cardiac development but normal hematopoiesis in mice deficient in the second CXCL12/SDF-1 receptor, CXCR7. Proc Natl Acad Sci U S A. 2007 Sep 11.104:14759. [PubMed: 17804806]

28. Shimizu H, Yamamoto K. NF-kappa B and C/EBP transcription factor families synergistically function in mouse serum amyloid A gene expression induced by inflammatory cytokines. Gene. 1994 Nov 18.149:305. [PubMed: 7959007]

29. Hu X, et al. Sensitization of IFN-gamma Jak-STAT signaling during macrophage activation. Nat Immunol. 2002 Sep.3:859. [PubMed: 12172544]

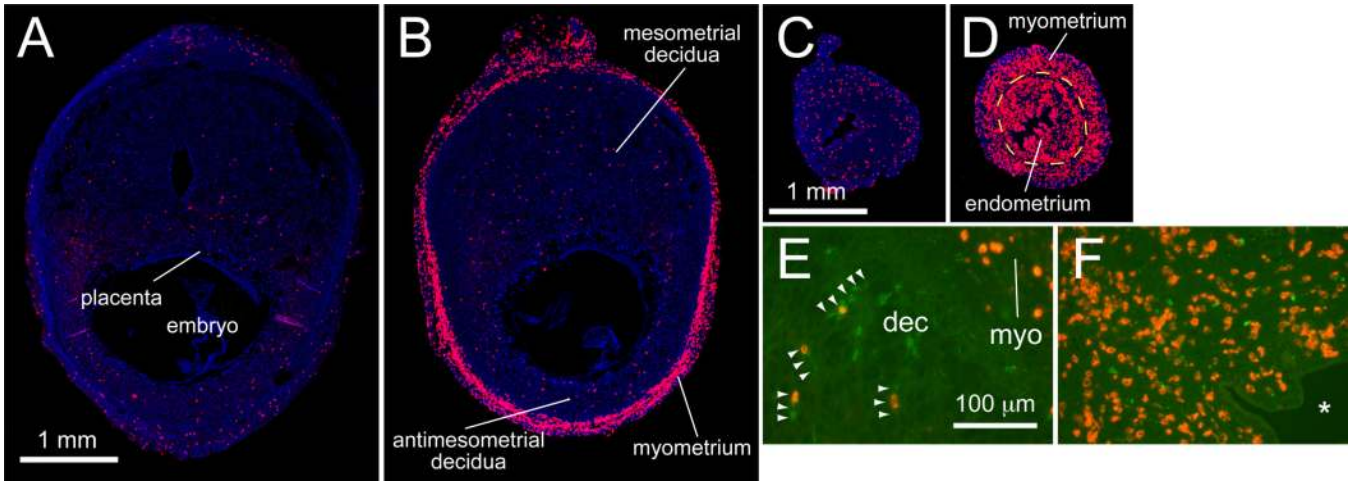

Fig. 1.

The decidua resists infiltration by reactivated memory T cells. (A–D) B6CBAF1/J (H-$2^{b/k}$) females were given 3×10^5 OVA-specific OT-I $CD8^+$ T cells, in order to maximize potential T cell accumulation, and immunized with OVA protein 2–3 weeks prior to mating to C57BL/6 males. On E5.5, pregnant mice either received no additional treatment (A, C) or were intravenously injected with 0.5 mg OVA and adjuvant (CD40 antibodies plus poly(I:C)) (B, D). The mice were sacrificed on E8.5, and tissue immunostaining using CD3-specific antibodies (red) was performed on cross-sections of implantation sites (A, B) and inter-implantation sites (C, D). The two poles of the decidua (mesometrial and anti-mesometrial) are indicated. DAPI counterstain. (E, F) The decidual/myometrial border (E) and undecidualized endometrium (F) of a rechallenged mouse. Blood vessels (arrowheads) are identified by the presence of RBCs, which appear green as an artifact of the immunostaining protocol. myo, myometrium; dec, decidua; asterisk, uterine lumen. Data are representative of N=3 independent experiments (at least n=23 implantation sites each per group).

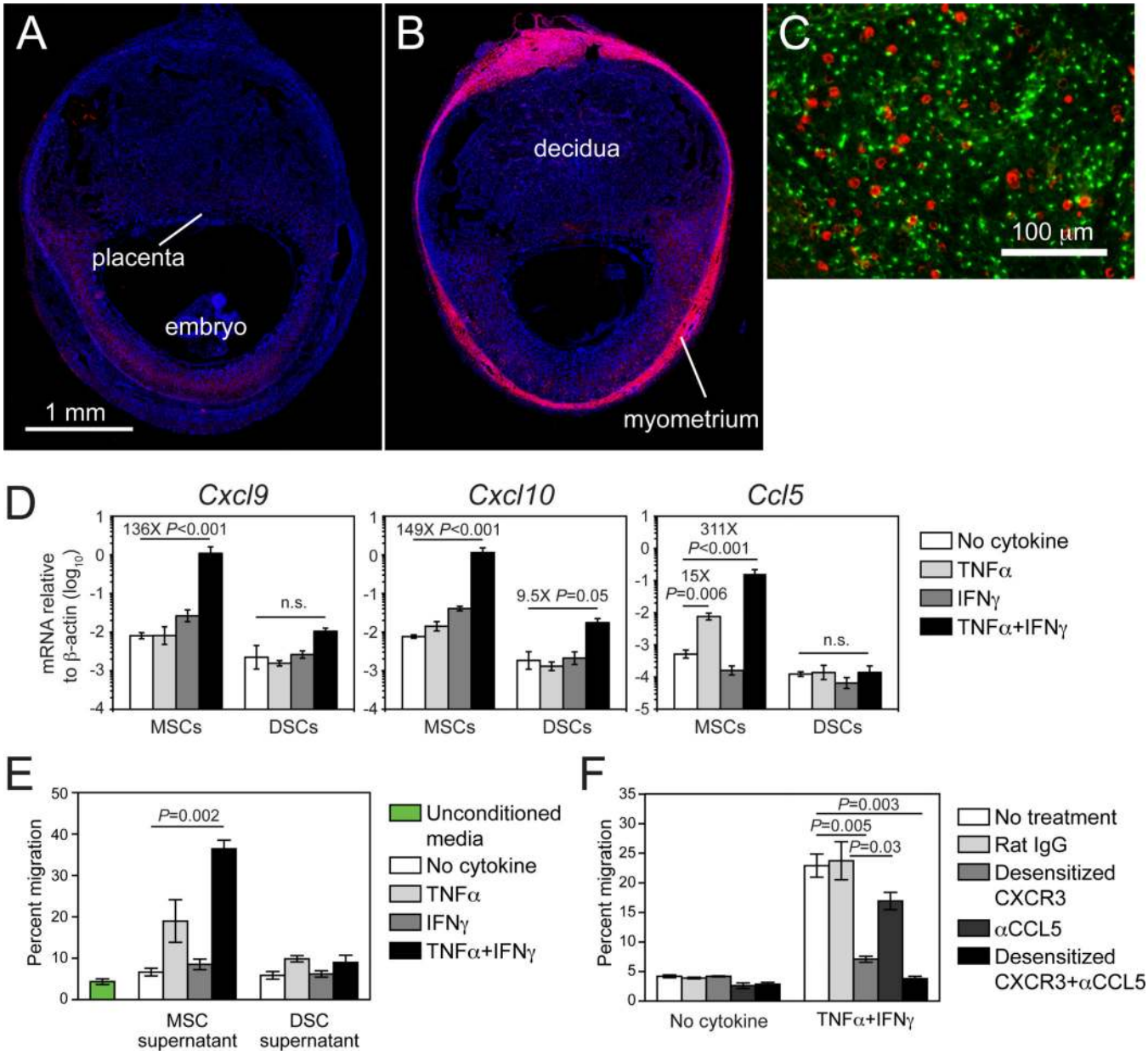

Fig. 2.

The decidua produces low levels of Th1/Tc1-attracting chemokines in response to inflammation. (A–C) E8.5 pregnant (A, B) or pseudopregnant (C) B6CBAF1/J mice were either untreated (A) or injected with CD40 antibodies, poly(I:C), and OVA (B, C) 6 h prior to sacrifice. (A, B) CXCL9 immunostaining (red) of implantation site cross-sections. (C) Double CXCL9 (green)/CD45 (red) immunostaining of the endometrium of an inflamed pseudopregnant uterus. CXCL9 immunoreactivity appears largely confined to the endoplasmic reticulum, giving a punctate appearance. Data are representative of at least *N*=3 independent experiments. DAPI counterstain. (D) qRT-PCR analysis of cultured MSCs and DSCs. Cytokines were added for the last 6 h of a 24 h total culture period. Data show mean ±SEM of *N*=4 independent experiments. n.s., not significant. (E) Migration of *in vitro* differentiated Th1 cells to supernatants collected from MSCs or DSCs treated as indicated over the entirety of a 24 h culture period. Data show mean±SEM of *N*=3 independent

experiments. (F) Effect of CXCR3 desensitization (via pre-incubation of the Th1 cells with CXCL9) or CCL5 neutralization on Th1 cell migration to supernatants from TNFα+IFNγ-treated MSCs. Non-specific rat IgG antibodies served as the control for CCL5 antibodies. Data show mean±SEM of N=3 independent experiments.

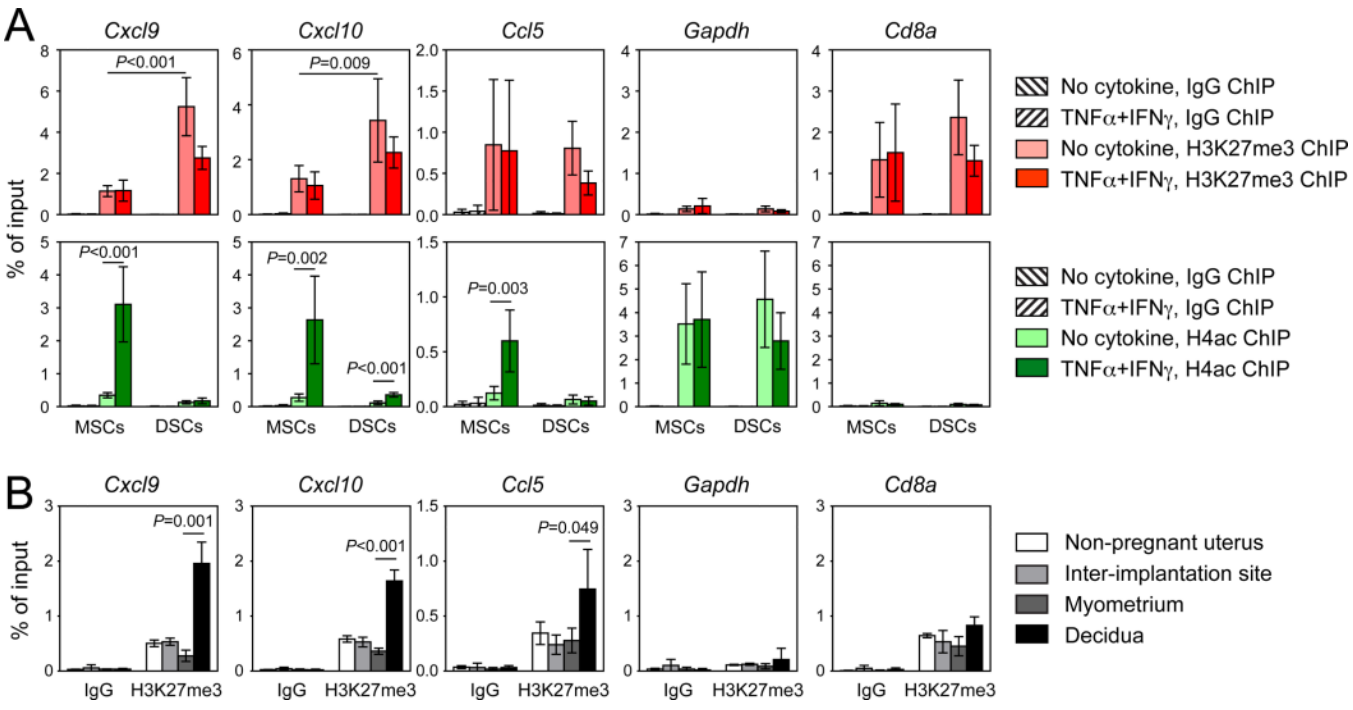

Fig. 3.

Chromatin configurations in uterine cells and tissue layers. (A) *Ex vivo* ChIP assays performed on cultured MSCs and DSCs. Cytokines were added for the last 6 h of a 24 h total culture period. Data show mean±SD of *N*=5 independent experiments. (B) *In vivo* ChIP assays performed on dissected uterine tissues and tissue layers. Deciduas were dissected free of embryos. Data show mean±SD of *N*=3 independent experiments.

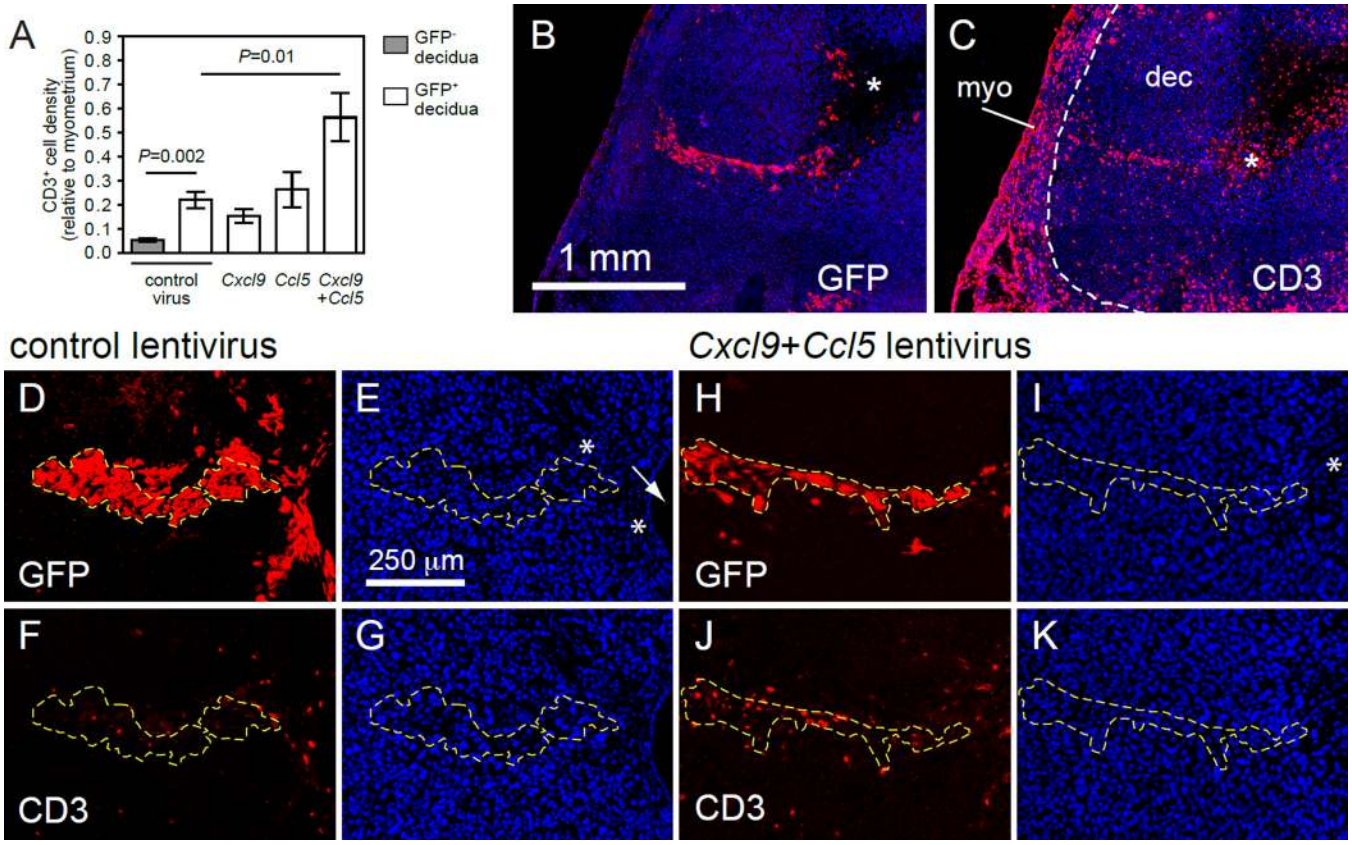

Fig. 4.

Effect of ectopic chemokine expression on effector T cell accumulation within the decidua. Mice were immunized with OVA 2–3 weeks prior to mating, rechallenged with OVA plus adjuvants on E4.5, injected with lentivirus on E5.5, and sacrificed on E7.5. Viral preparation included aliquots of EGFP reporter lentiviruses so that T cells within transduced areas could be identified on anti-CD3 and anti-GFP immunostained serial sections. (A) $CD3^+$ cell densities in infected (GFP^+) and uninfected (GFP^-) decidual areas relative to myometrial $CD3^+$ cell densities. Data show mean±SEM of at least N=3 independent experiments encompassing n=4 control (empty vector) virus-infected mice (75×10^7 virus particles each), n=5 *Cxcl9+Ccl5* virus-infected mice (37.5×10^7 particles each), and n=3 each of mice infected with *Cxcl9*- or *Ccl5*-expressing viruses alone (75×10^7 particles each). Myometrial $CD3^+$ cell densities were not significantly different between the four groups (average: 0.037 cells/μm^2). (B–K) GFP or CD3 immunostaining (as indicated, red) and DAPI counterstain (blue) of representative serial sections of decidualized uteri infected with *Cxcl9+Ccl5* viruses (B–C, H–K) or control viruses (D–G). B and C: asterisks denote different areas of the decidual lumen, which frequently contained GFP^+ cells, $CD3^+$ cells, and granulocytes scattered among necrotic debris; the dashed line indicates the border between the myometrium and decidua. D–K: the dashed lines show the perimeters of infected areas used to calculate $CD3^+$ cell densities; asterisks show areas excluded from analysis because of their necrotic appearance. Arrow, decidual lumen. Panels H–K are close-ups of B and C.